HHS Public Access

Author manuscript

Transl Stroke Res. Author manuscript; available in PMC 2021 June 01.

Published in final edited form as:

Transl Stroke Res. 2020 June ; 11(3): 541–551. doi:10.1007/s12975-019-00745-4.

CD47 blocking antibody accelerates hematoma clearance after intracerebral hemorrhage in aged rats

Chuanyuan Tao, MD, PhD.[1,2], **Richard F. Keep, Ph.D.**[1], **Guohua Xi, MD**[1], **Ya Hua, MD**[1]

[1]Department of Neurosurgery, University of Michigan, Ann Arbor, Michigan, USA

[2]Department of Neurosurgery, West China Hospital, Sichuan University, Chengdu, China

Abstract

Both experimental studies and surgical clinical trials suggest that hematoma clearance has is a therapeutic target in intracerebral hemorrhage (ICH). We have investigated effects of CD47, a 'don't eat me' signal expressed on erythrocytes, on hematoma resolution after ICH in young mice. This study expands those findings by examining the effects on a CD47 blocking antibody in aged rats. First, male Fischer 344 rats (18 months old) received an intracaudate injection of 50μL autologous whole blood or saline. Hematoma features of magnetic resonance imaging (MRI) and neurological deficits were evaluated within 3 days. Second, rats had an intracaudate co-injection of 50μL autologous blood with either CD47 blocking antibody or IgG. MRI was used to quantify hematoma/iron volume, hemolysis, brain swelling and atrophy at different time points, behavioral tests to assess neurological deficits and immunohistochemistry to assess brain injury and neuroinflammation. The CD47 blocking antibody significantly promoted hematoma clearance, attenuated brain swelling, hemolysis and neuronal loss and increased the number of phagocytic macrophages in and around hematoma 3 days after ICH. Moreover, CD47 blockade reduced neuronal loss, brain atrophy and neurobehavioral deficits at day 28. These results indicate that a CD47 blocking antibody can accelerate hematoma clearance and alleviate short- and long-term brain injury after ICH in aged rats and that it might be a therapeutic strategy for ICH.

Keywords

CD47 blocking antibody; cerebral hemorrhage; macrophage activation; aged rats

Introduction

Hematoma size is the strongest predictor of patient outcome after intracerebral hemorrhage (ICH)[1]. Hematoma size will impact both the initial mass effect and the release of potentially neurotoxic factors from red blood cells (RBCs)[2]. Hence, hematoma reduction represents a

Correspondence: Ya Hua, M.D., R5018 BSRB, University of Michigan, 109 Zina Pitcher Place, Ann Arbor, Michigan 48109-2200, USA, Telephone: +1 (734) 764-1207, Fax: +1 (734) 763-7322, yahua@umich.edu.

Compliance with Ethical Standards

Conflict of Interests: Chuanyuan Tao, Richard F. Keep, Guohua Xi, and Ya Hua declare no conflict of interests.

Ethical approval: All institutional and national guidelines for the care and use of laboratory animals were followed.

key target in ICH treatment[3]. However, surgical hematoma evacuation failed to improve functional outcomes in ICH patients probably because of insufficient hematoma removal[4]. An alternative or complementary approach is to accelerate endogenous mechanisms involved in hematoma clearance[3]. Thus, stimulating phagocytosis via microglia/macrophage (M/MΦ) activation with peroxisome proliferator-activated receptor-γ agonists accelerates hematoma clearance in murine ICH models[2, 5, 6].

CD47, a glycoprotein, is expressed on RBC membranes and acts as a “don’t eat me” signal. Low CD47 levels are present on senescent RBCs and are associated with increased macrophage clearance[7]. Our previous studies showed that erythrophagocytosis in the hematoma was related to reduced clot CD47 levels in a piglet ICH model[8], and that CD47 gene deletion[9] or use of a blocking CD47 antibody[10] augmented hematoma clearance in mouse ICH models and this was associated with less brain swelling, neuronal death and neurological deficits. However, there are significant differences in immune responses between mice and rats[11, 12]. For example, the resting/stimulated expression of microglial markers (Iba1, CD11b, CD68) differs between the species[11]. Moreover, those species show distinct and even opposite changes in the expression of M1 or M2 markers when primary microglia are stimulated by the same pro- or anti-inflammatory mediators[11]. Therefore, evidence from mice may not be generalizable to rats and other species.

Age is an independent factor affecting ICH prognosis and ICH is mostly a disease of the elderly. Evidence suggests that aging exerts vital effects on RBCs and phagocytic cells. Thus, in old animals and humans, RBCs have a shorter lifespan[13, 14] and aging was reported to reduce the phagocytic capacity of M/MΦ *in vitro*[15, 16]. Therefore, the effect of CD47 on hematoma clearance should be examined in aged animals for better translational research.

The aim of the present study was, therefore, to examine the effect of a CD47 blocking antibody on hematoma resolution in aged rats. It also examined whether that antibody improved short- and long-term brain injury and neurological deficits in those animals.

Material and Methods

Animals and ICH

The protocols for the animal use were approved by the University of Michigan Institutional Animal Care and Use Committee. The study complies with the ARRIVE guidelines for reporting in vivo experiments. Randomization was carried out using odd/even numbers. A total of 81 male aged Fischer 344 rats (age: 18 months; weight: 390–470 grams; NIH) were used in the study. To create the ICH model, rats were anesthetized with pentobarbital (40 mg/kg; i.p.) and positioned in a stereotactic frame (Kopf Instruments, Tujunga, CA). Body temperature was kept at 37°C using a feedback-controlled heating pad. After a midline scalp incision, a 1 mm diameter cranial burr hole was drilled on the right coronal suture 3.5mm lateral to the midline. A 26-gauge needle was inserted into the right caudate (coordinates: 0.2 mm anterior, 5.5 mm ventral and 3.5 mm lateral to the bregma) and autologous whole blood (50μl) obtained from right femoral artery, or equal amount of saline was injected at a rate of 10μl/min using a microinfusion pump (Harvard Apparatus Inc.). The needle was then removed, the burr hole filled with bone wax and the skin sutured.

Experimental groups

There were three parts to this study. In the first part, rats had an intracaudate injection of 50μl blood (n=7) or saline (n=6). MRI scanning and neurobehavioral evaluation were performed at days 1 and 3 after ICH. Rats were euthanized at 3 days after surgery. In the second part, rats received an intracaudate injection of 50μl blood mixed with either anti-CD47 antibody (n=18) or IgG (n=17). Specifically, 3μl (0.3ug) anti-CD47 antibody or IgG was mixed gently in 300μl blood. All rats underwent MRI scanning and behavioral testing at day 1 and 3. Brains were harvested for histology at day 3. In the third part, rats had an intracaudate injection of 50μl blood with anti-CD47 antibody (n=17) or IgG (n=16). All rats had MRI and behavioral tests at days 1, 3, 7 and 28. Rats were euthanized for brain histology at days 28.

Nine rats died during surgery with 1 in the ICH, 3 in the ICH+anti-CD47 antibody and 5 in the ICH+IgG groups. One rat in the ICH+anti-CD47 antibody group was excluded due to cerebral infection. Eight rats were excluded due to small hematoma size (< 5μl) on T2* imaging at day 1 (4 in the ICH+anti-CD47 antibody and 4 in the ICH+IgG group). Three rats were excluded for occurrence of acute hydrocephalus evaluated on T2 imaging at day 3 (2 in the ICH+anti-CD47 antibody and 1 in the ICH+IgG group).

Hydrocephalus development after ICH may be related to ventricular extension of hemorrhage. Ventricular extension of hemorrhage also resulted in small hematomas. Since we used ipsilateral ventricular compression at day 3 to estimate brain swelling and ipsilateral ventricular dilation at day 28 to estimate brain atrophy, animals with hydrocephalus were excluded in this experiment.

MRI measurements

Rats underwent MRI in a 9.4-Tesla MR scanner at different time-point following ICH. During scanning, rats were anesthetized with a 2% isoflurane and air mixture. The imaging protocol included a T2 fast spin-echo and T2* gradient echo sequences with the following parameters: repetition time (TR) = 4000ms and effective echo time (TE) = 60ms for T2 imaging, TR = 250ms and TE = 5ms for T2* imaging. Other parameters included field of view (FOV) = 35 × 35 mm, matrix = 256 × 128 and slice thickness = 0.5mm for both T2 and T2* imaging.

While T2* lesion volume is a measure of hematoma size at acute stage (day 1 and day 3), it correlates with iron deposition at later time (day 28) when the hematoma resolves[17]. The T2* lesion was outlined on all slices and the lesion volume determined by combining the total areas and multiplying by section thickness (0.5 mm) using NIH Image J. The difference between T2* lesion volumes at day 3 and 1 divided by the lesion volume at day 1 was used to calculate the % reduction in hematoma volume over that time period. Similarly, the difference in T2* lesion volume at day 28 (a measure of brain iron deposition) and the T2* lesion volume at day 1 (a measure of initial hematoma volume) divided by the T2* lesion volume at day 1 was calculated as a measure of iron clearance from brain.

Early hemolysis was detected on T2*-weighted imaging. As previously described[18], the iso- and hyper-intense signal area in hematoma center was outlined on every slice, and the iso/

hyperintense signal volumes were obtained as the non-hypo-T2* lesion. The ratio of non-hypo-T2* lesion volume to total T2* lesion volume was quantified to assess hemolysis at day 1 and days 3 after ICH.

The ratio of ipsilateral to contralateral ventricular size was measured to evaluate brain swelling (ventricular compression due to the hematoma and brain edema) at day 3 and brain atrophy at day 28. Therefore, only brain swelling rather than brain edema was measured in this study. In the ICH model with small hematomas, we didn't find marked midline shift. The ratio of ipsilateral to contralateral ventricular size was measured to evaluate brain swelling (ventricular compression due to the hematoma and brain edema) at day 3. At day 28, hematomas have been resolved. The enlargement of the ipsilateral ventricle after hematoma clearance can be used to estimate brain tissue loss after ICH. Three MRI slices on T2-weighted images, centered on the needle track layer, were chosen to outline the bilateral ventricles and each ventricle size was obtained. We used T2* images to determine hemolysis in the hematomas at day 1 and day 3. T2 images were only used for brain atrophy measurements at day 28. The difference in T2* lesion volume at day 28 (a measure of brain iron deposition) and the T2* lesion volume at day 1 (a measure of initial hematoma volume) divided by the T2* lesion volume at day 1 was calculated as a measure of iron clearance from brain.

Brain Histology and H&E Staining

Rats were euthanized with pentobarbital and underwent trans-cardiac perfusion with 4% paraformaldehyde. Brains were sectioned on a cryostat (18-μm-thick slices). Hematoxylin and eosin (H&E) staining was performed following a standard protocol and used to demarcate the hematoma.

Immunohistochemistry and Immunofluorescence Double Labeling

Immunohistochemistry staining and immunofluorescence double labeling were performed as previously described[9, 19]. The primary antibodies were mouse anti-CD68 (Abcam, ab31630, 1:100), rabbit anti-heme oxygenase-1 (HO-1, Enzo, ADI-SPA-895-F, 1:400), rabbit anti-ferritin (Sigma, F5012, 1:400) and rabbit anti-dopamine- and cAMP-regulated phosphoprotein, Mr 32 kDa (DARPP-32, CST, 2306s, 1:200). Negative controls were normal mouse IgG, rabbit IgG or eliminated the primary antibody. Secondary antibodies were horse anti-mouse (Vector laboratories inc, BA-2001, 1:400), goat anti-rabbit (Invitrogen, #31820, 1:400), donkey anti-mouse (Invitrogen, Alexa Fluor TM 594 IgG, 1:500) and donkey anti-rabbit (Invitrogen, Alexa Fluor TM 488 IgG, 1:500). DARPP-32 is a marker of striatal neurons. Neuronal loss in the caudate was determined by DARPP-32 loss (contralateral - ipsilateral)/contralateral × 100%.

Enhanced Perls' staining

Perls' staining for iron was performed as previously described[20]. In brief, brain sections were incubated in Perls' solution (1:1, 5% potassium ferrocyanide and 5% HCl) for 10 minutes. After washing in distilled water, sections were immersed in 0.5% diamine benzidine tetrahydrochloride with nickel for another 6 minutes.

Cell Counting

Cell counting was performed on brain coronal sections in a blinded manner. High power images (×40 magnification) were taken from the hematoma and perihematomal areas. Three slides from each brain with each slide containing three fields of interest in the hematoma or perihematomal areas were digitized. All measurements were repeated three times and the mean value used.

Behavioral tests

Corner turn and forelimb use asymmetry tests were used to assess neurological deficits as described previously[21]. For the forelimb limb-use asymmetry test, forelimb use during rat explorative activity in a transparent cylinder was analyzed. Behavior was quantified by determining the events when the non-impaired (Ipsilateral to the hematoma site) forelimb was used (I), he events when the impaired forelimb (Contralateral to the hematoma site) was used (C), and the events when "both" forelimbs were used simultaneously (B). Limb use asymmetry score = (I/(I+C+B)) - (C/(I+C+B)). For corner turn test, the rat was allowed to proceed into a corner, the angle of which was 30 degrees. To exit the corner, the rat turned either to the left or the right. This was repeated 10 times, and the percentage of right turns was calculated. All rats were tested before surgery and at different time points after surgery. A blinded investigator performed behavioral tests.

Statistical Analysis

All values are expressed as mean ± SD. Data were analyzed with Student's *t* test and one- or two-way ANOVA test with a Bonferroni multiple comparisons test when needed. Significance levels were set at $P < 0.05$.

Results

Characteristics of ICH induced by intracaudate injection of 50μl autologous whole blood

Our prior studies have focused on using a 100μl injection of autologous blood into the caudate of the rat so we first characterized the effects of the 50μl blood injection in aged rats using MRI and behavioral testing. The average volume of T2* lesion was 18.7±4.6μl at day 1, increased to 20.8±4.8μl at day 3 (Figure 1A). Hemolysis was detected and quantified on T2*-weighted imaging. The ratio of non-hypo-T2* lesion volume to total T2* lesion volume was 3.8±0.7 and 4.9±1.2 % at days 1 and day 3 (n=6; Figure 1A).

ICH led to ipsilateral ventricular compression (ipsilateral/contralateral ventricular volume <100%) at day 1, a measure of brain swelling due to hematoma and edema. This reduction in ventricle size was significantly greater (50.5±14.0 %, n=6) than in saline-injected rats (75.9±16.6 %, n=6, P< 0.05, Figure 1B) and it was maintained at day 3 after ICH (49.1±17.9 %, n=6).

ICH also resulted in significant acute neurological deficits. The corner turn score was 100±0 % (n=6) vs. 85±16 % (n=6) in saline group at day 1 (P< 0.05) and 93±8% (n=6) vs. 62±12 % (n=6) in saline group at day 3 (P< 0.05). Similarly, the forelimb asymmetry use score was 78±26 % (n=6) vs. 22±22 % (n=6) in saline group at day 1 (P< 0.05) and 68±26 % (n=6) vs.

16±14 % (n=6) in saline group at day 3 (P< 0.05, Figure 1C). Collectively, the 50μl blood injection model is able to produce consistent hematoma, hemolysis, brain swelling and neurological deficits.

CD47 blocking antibody promoted hematoma clearance

Hematoma clearance was determined from T2* lesion changes. At day 1, there was no significant difference in T2* lesion volume between anti-CD47 antibody and IgG co-injected groups (19.4±6.7μl, n=25 vs. 18.8±6.7μl, n=23; P> 0.05, Figure 2A). At day 3, the T2* lesion continues to match the hematoma found on H&E staining (Figure 2B) and changes in T2* lesion volume between day 1 and 3 were assessed to examine if the CD47 blocking antibody affected hematoma size. To normalize for differences in initial hematoma volume changes were calculated as day ((3 lesion volume – day 1 lesion volume)/day 1 lesion volume)*100%. The CD47 blocking antibody significantly accelerated clearance at day 3 (−2.6±16.4%, n=25 vs. 13.0±14.6%, n=23 in IgG group, P< 0.01, Figure 2B).

By day 28, the T2* lesion and Perls' staining for iron deposition delineate the same brain area (Figure 2C). In the CD47 blocking antibody group, the T2* lesion volume at 28 days was 32.5±14.5% smaller than the T2* lesion volume at day 1 (n=13). In the IgG control group, it was 24.7±11.3% smaller (n=12, Figure 2C). These reductions were not significantly different (P>0.05).

CD47 blockade alleviated brain swelling, brain atrophy and neurological deficits

Brain swelling, brain atrophy and neurological deficits develop after ICH. The ratio of ipsilateral to contralateral ventricular size was used to assess brain swelling or atrophy depending on the time point. Ventricular compression, due to hematoma volume and edema, was noted at day 3 and ventricular enlargement, due to brain atrophy, occurred at day 28. CD47 blockade significantly reduced brain swelling at day 3 (ipsilateral ventricle/contralateral: 70.6±13.7%, n=25 vs. 48.3±17.3%, n=23 in IgG treated rats, P< 0.01, Figure 3A) and brain atrophy at day 28 (127±28%, n=13 vs. 160±34%, n=12 in IgG treated rats, P< 0.01, Figure 3B).

Corner turn and forelimb use asymmetry tests were performed to evaluate neurological deficits. No differences were observed at pretest, day 1, 3 and 7 after ICH between CD47 blocking antibody and IgG treatment groups. However, CD47 blocking antibody significantly improved neurological function at day 28 as assessed by corner turn test (57±11 %, n=13 vs. 74±16 %, n=12 in IgG group, P< 0.05, Figure 3C) and forelimb asymmetry use score (28±29 %, n=13 vs. 55±16 %, n=12 in IgG group, P< 0.05, Figure 3D).

CD47 blocking antibody alleviated early hemolysis

Our previous study found that early hemolysis in the hematoma occurs after ICH which is correlated with perihematomal neuronal loss[18]. The ratio of non-hypo-T2* lesion volume to total T2* lesion volume was used to quantify hemolysis at days 1 and 3. The ratio was significantly decreased after CD47 blocking antibody co-injection at day 1 (2.1±1.4 %, n=25

vs. 3.2±1.3 %, n=23 in IgG group, P< 0.01, Figure 4A) and day 3 (3.2±1.3 %, n=25 vs. 4.3±1.5 %, n=23 in IgG group at day 3, P< 0.05, Figure 4B).

CD47 blocking antibody reduced neuronal loss

DARPP-32 is a specific marker of neurons in striatum. Anti-CD47 antibody significantly reduced neuronal loss at day 3 (8.6±4.0 %, n=12 vs. 13.4±5.2 %, n=11 in IgG group at day 1, P< 0.05; Figure 5A) and day 28 (10.9±5.9 %, n=9 vs. 19.4±6.5 %, n=8 in IgG group at day 1, P< 0.05; Figure 5B).

CD47 blocking antibody activated phagocytic M/MΦ

Phagocytosis by activated M/MΦ is important in hematoma clearance[5]. CD68 is a marker of activated M/MΦ. At day 3, CD68 positive cells were significantly increased by the co-injection of anti-CD47 antibody in the hematoma (342±86/mm^2, n=12 vs. 245±117/mm^2, n=11 in IgG group, P< 0.05) as well as in the perihematomal region (1021±313/mm^2, n=12 vs. 687±154/mm^2, n=11 in IgG group, P< 0.01; Figure 6A).

Heme oxygenase-1 (HO-1) is a key enzyme in heme degradation[22] while ferritin an iron-storage protein in M/MΦ[20] and heme and iron detoxification is important in limiting ICH-induced brain injury[22]. Immunofluorescent double labeling showed that more than 85% CD68-positive cells were HO-1 in the hematoma core and in the perihematomal area in the anti-CD47 antibody group, while nearly 80% CD68 positive cells were also stained with ferritin in and around hematoma (Figure 6B).

Discussion

The current study found that: 1) ICH with 50μl blood intracaudate injection resulted in remarkable brain injury in aged rats; 2) CD47 blocking antibody promoted hematoma clearance at day 3 compared to controls; 3) the blocking antibody also alleviated acute brain swelling, hemolysis and neuronal loss as well as long-term neuronal loss, brain atrophy and neurological deficits; 4) it also increased the number of activated phagocytic M/MΦ in and around the hematoma, which may take part in erythrocyte engulfment and metabolism.

Hematoma size is a key factor determining outcomes in ICH patients[1]. This may relate to the greater initial mass effect of the hematoma and the greater reservoir of potential neurotoxic factors such as hemoglobin and iron[22]. There has, therefore, been interest in developing methods to reduce hematoma volume. Recently, MISTIE III, an international multicenter randomized clinical trial, identified an association between the extent of blood reduction and improved functional outcome[4], supporting the concept that enhancing hematoma clearance may limit ICH-mediated brain injury. Our previous work indicated that loss of CD47 on RBCs accelerated hematoma resolution in mice[9]. Moreover, we recently found that an anti-CD47 antibody, which can block CD47 on RBC, accelerated hematoma clearance and alleviated brain injury when co-injected with blood in mice[10]. In this study, we further validated the effect of anti-CD47 antibody in aged rats, indicating that CD47 may be a therapeutic target in ICH. The potential benefit of blocking CD47 was further supported by reduced neuronal loss, brain atrophy and neurological deficits. It should be noted there are marked differences in the immune system between rodents and humans. In future

translational studies, large animals (e.g. pigs) should be used to confirm the efficacy of CD47 blocking antibody in affecting hematoma clearance.

Using serial MRI to examine hematoma clearance is complicated by several factors. T2* imaging will detect hematoma but also iron deposition that occurs after hematoma clearance as noted by the comparison between our T2* images at day 3, which correspond to hematoma found on H&E staining, and at day 28, where they correspond to iron deposition found on Perls' staining. In addition, in this study we found that in the IgG-treated group, the hematoma expanded slightly between day 1 and 3. Thus, our description of accelerated clearance in the CD47 antibody-treated group is against that background. The data at day 28 did not show a significant difference in T2* lesions between the IgG- and CD47 antibody-treated groups. This raises an important issue, the fate of iron after M/MΦ-mediated phagocytosis of the hematoma and whether accelerated phagocytosis alters that distribution (e.g. will all iron in the hematoma ultimately be deposited as perihematomal hemosiderin or does some iron leave the brain)?

The current study employed a 50μl blood injection in rats. A 50μl hematoma in rat brain approximates 22 ml blood in human brain when the whole brain volume of 2.7ml in rat[23] and 1200ml in human[24] are taken into account. The current ICH model may mimic the small residual hematomas after surgical clot evacuation in patients. For example, only 58% surgical patients in MISTIE III achieved the prespecified surgical goal of ≤15ml residual clot volume[4]. A combination therapy with anti-CD47 antibody administration after surgical hematoma removal might be promising after ICH.

Hemolysis may be a vital contributor to brain injury after ICH[25]. We previously found that early hemolysis occurred in hematoma center which correlated with the severity of perihematomal neuronal death[18], and that inhibiting hemolysis alleviated ICH-induced neuronal death and neurological deficits[26]. Further, increased hemolysis is expected in aged rats as a result of higher complement activation in comparison with younger rats[27]. In the present study, anti-CD47 antibody decreased hemolysis at days 1 and 3. This may be by promoting erythrophagocytosis before erythrolysis happens. Other mechanisms underlying anti-CD47 antibody-induced reduction of hemolysis remain to be explored. However, hematoma volume is a crucial determinant of hemolysis. Our previous study[18] showed that the ratio of hemolysis to hematoma was 16% at day 1 and 21% at day 3 in 100μl whole blood injection model, which is much higher than that in the current ICH model with approximately 5% within 3 days. It will be interesting to examine the effect of CD47 blocking antibodies on hemolysis in larger hematomas.

Aging has multiple effects on neurons, microglia, astrocytes, lesion size, brain atrophy, and neurological deficits after experimental ICH[28–30]. However, the effect of aging on hematoma resolution remains to be clarified. Hematoma clearance is influenced by the properties of both phagocytic cells and RBCs. During their lifespan, RBCs express less CD47 which is associated with the clearance of senescent erythrocytes[31]. On the other hand, we have found an increased M/MΦ response at day 3 in aged compared to young rats following ICH[30]. However, such studies have focused on the numbers of activated M/MΦ, and whether phagocytic function is really enhanced in aging ICH animals remains unknown. In fact, it

has been reported that there is an increased basal but reduced induced phagocytic and lysosomal activity of microglia in aged brain[32].

CD68, also named ED1, predominantly locates in endosomes and lysosomes of M/MΦ. CD68 is generally recognized as a marker of activated M/MΦ after ICH[28, 33–35]. However, whether CD68 plays critical roles in erythrophagocytosis remains to be investigated. Iba-1 labeled M/MΦ have been categorized into 3 phenotypes according to their morphology after ICH in aged rats: ramified, activated and macrophage-like[28]. Macrophage-like M/MΦ are round without obvious cell processes, functioning as phagocytes[28]. In our study, all CD68 positive cells were of macrophage-like shape, suggesting that CD68 is involved in phagocytosis. Moreover, most CD68 positive cells co-labeled with HO-1 and ferritin, suggesting that those cells were involved in handling erythrocyte degradation products. In support a role of CD68 in phagocytosis, it has been considered as a scavenger receptor type D as it can bind modified low-density lipoprotein, phosphatidylserine, and apoptotic cells[36].

There are several limitations in the current study: 1) the results from our smaller ICH model may not be generalizable to all sizes of ICH; 2) only one dose of the CD47 blocking antibody was tested and the optimal dose should be further determined; 3) it does not examine the effect of delayed treatment; 4) the effect of the CD47 blocking antibody in female aged rats needs to be examined in future studies; 5) only brain swelling rather than brain edema was measured; and 6) it is unclear whether CD47 blocking antibody will be cleared in the hematoma within days and whether CD47 blocking antibody should given multiple times to enhance hematoma resolution.

Conclusions

A CD47 blocking antibody accelerated hematoma clearance and alleviated acute and chronic brain injury after ICH in aged rats. This was associated with increased macrophage activation. CD47 may be a potential therapeutic target in ICH.

Acknowledgments

Funding: YH, RFK and GX were supported by grants NS-090925, NS-096917, NS-106746 and NS-112394 from the National Institutes of Health.

References

1. Broderick JP, Brott TG, Duldner JE, Tomsick T, Huster G. Volume of intracerebral hemorrhage. A powerful and easy-to-use predictor of 30-day mortality. Stroke. 1993;24:987–993 [PubMed: 8322400]
2. Zhao X, Sun G, Ting SM, Song S, Zhang J, Edwards NJ, et al. Cleaning up after ich: The role of nrf2 in modulating microglia function and hematoma clearance. J Neurochem. 2015;133:144–152 [PubMed: 25328080]
3. Wilkinson DA, Keep RF, Hua Y, Xi G. Hematoma clearance as a therapeutic target in intracerebral hemorrhage: From macro to micro. J Cereb Blood Flow Metab. 2018;38:741–745 [PubMed: 29350086]
4. Hanley DF, Thompson RE, Rosenblum M, Yenokyan G, Lane K, McBee N, et al. Efficacy and safety of minimally invasive surgery with thrombolysis in intracerebral haemorrhage evacuation (mistie iii): A randomised, controlled, open-label, blinded endpoint phase 3 trial. Lancet. 2019;393:1021–1032 [PubMed: 30739747]

5. Zhao X, Sun G, Zhang J, Strong R, Song W, Gonzales N, et al. Hematoma resolution as a target for intracerebral hemorrhage treatment: Role for peroxisome proliferator-activated receptor gamma in microglia/macrophages. Ann Neurol. 2007;61:352–362 [PubMed: 17457822]
6. Wang G, Li T, Duan SN, Dong L, Sun XG, Xue F. Ppar-gamma promotes hematoma clearance through haptoglobin-hemoglobin-cd163 in a rat model of intracerebral hemorrhage. Behav Neurol. 2018;2018:7646104 [PubMed: 30123388]
7. Oldenborg PA, Zheleznyak A, Fang YF, Lagenaur CF, Gresham HD, Lindberg FP. Role of cd47 as a marker of self on red blood cells. Science. 2000;288:2051–2054 [PubMed: 10856220]
8. Cao S, Zheng M, Hua Y, Chen G, Keep RF, Xi G. Hematoma changes during clot resolution after experimental intracerebral hemorrhage. Stroke. 2016;47:1626–1631 [PubMed: 27125525]
9. Ni W, Mao S, Xi G, Keep RF, Hua Y. Role of erythrocyte cd47 in intracerebral hematoma clearance. Stroke. 2016;47:505–511 [PubMed: 26732568]
10. Jing C, Bian L, Wang M, Keep RF, Xi G, Hua Y. Enhancement of hematoma clearance with cd47 blocking antibody in experimental intracerebral hemorrhage. Stroke. 2019;50:1539–1547 [PubMed: 31084334]
11. Lam D, Lively S, Schlichter LC. Responses of rat and mouse primary microglia to pro- and anti-inflammatory stimuli: Molecular profiles, k(+) channels and migration. J Neuroinflammation. 2017;14:166 [PubMed: 28830445]
12. Wei J, Wu F, Sun X, Zeng X, Liang JY, Zheng HQ, et al. Differences in microglia activation between rats-derived cell and mice-derived cell after stimulating by soluble antigen of iv larva from angiostrongylus cantonensis in vitro. Parasitol Res. 2013;112:207–214 [PubMed: 23073569]
13. Magnani M, Rossi L, Stocchi V, Cucchiarini L, Piacentini G, Fornaini G. Effect of age on some properties of mice erythrocytes. Mech Ageing Dev. 1988;42:37–47 [PubMed: 3347096]
14. Shperling T, Danon D. Age population distribution of erythrocytes in young and old healthy donors. Exp Gerontol. 1990;25:413–422 [PubMed: 2257888]
15. Takahashi R, Totsuka S, Ishigami A, Kobayashi Y, Nagata K. Attenuated phagocytosis of secondary necrotic neutrophils by macrophages in aged and smp30 knockout mice. Geriatr Gerontol Int. 2016;16:135–142 [PubMed: 25597390]
16. von Bernhardi R, Tichauer J, Eugenin-von Bernhardi L. Proliferating culture of aged microglia for the study of neurodegenerative diseases. J Neurosci Methods. 2011;202:65–69 [PubMed: 21889955]
17. Zhao H, Garton T, Keep RF, Hua Y, Xi G. Microglia/macrophage polarization after experimental intracerebral hemorrhage. Transl Stroke Res. 2015;6:407–409 [PubMed: 26446073]
18. Dang G, Yang Y, Wu G, Hua Y, Keep RF, Xi G. Early erythrolysis in the hematoma after experimental intracerebral hemorrhage. Transl Stroke Res. 2017;8:174–182 [PubMed: 27783383]
19. Liu H, Hua Y, Keep RF, Xi G. Brain ceruloplasmin expression after experimental intracerebral hemorrhage and protection against iron-induced brain injury. Transl Stroke Res. 2019;10:112–119 [PubMed: 30315404]
20. Wu J, Hua Y, Keep RF, Nakamura T, Hoff JT, Xi G. Iron and iron-handling proteins in the brain after intracerebral hemorrhage. Stroke. 2003;34:2964–2969 [PubMed: 14615611]
21. Hua Y, Schallert T, Keep RF, Wu J, Hoff JT, Xi G. Behavioral tests after intracerebral hemorrhage in the rat. Stroke. 2002;33:2478–2484 [PubMed: 12364741]
22. Xi G, Keep RF, Hoff JT. Mechanisms of brain injury after intracerebral haemorrhage. Lancet Neurol. 2006;5:53–63 [PubMed: 16361023]
23. Pfefferbaum A, Adalsteinsson E, Sullivan EV. In vivo structural imaging of the rat brain with a 3-t clinical human scanner. J Magn Reson Imaging. 2004;20:779–785 [PubMed: 15503335]
24. Allen JS, Damasio H, Grabowski TJ. Normal neuroanatomical variation in the human brain: An mri-volumetric study. Am J Phys Anthropol. 2002;118:341–358 [PubMed: 12124914]
25. Liu R, Li H, Hua Y, Keep RF, Xiao J, Xi G, et al. Early hemolysis within human intracerebral hematomas: An mri study. Transl Stroke Res. 2019;10:52–56 [PubMed: 29766451]
26. Hatakeyama T, Okauchi M, Hua Y, Keep RF, Xi G. Deferoxamine reduces neuronal death and hematoma lysis after intracerebral hemorrhage in aged rats. Transl Stroke Res. 2013;4:546–553 [PubMed: 24187595]

27. Gong Y, Xi G, Wan S, Gu Y, Keep RF, Hua Y. Effects of aging on complement activation and neutrophil infiltration after intracerebral hemorrhage. Acta Neurochir Suppl. 2008;105:67–70 [PubMed: 19066085]
28. Wasserman JK, Yang H, Schlichter LC. Glial responses, neuron death and lesion resolution after intracerebral hemorrhage in young vs. Aged rats. Eur J Neurosci. 2008;28:1316–1328 [PubMed: 18973558]
29. Lee JC, Cho GS, Choi BO, Kim HC, Kim WK. Aging exacerbates intracerebral hemorrhage-induced brain injury. J Neurotrauma. 2009;26:1567–1576 [PubMed: 19473060]
30. Gong Y, Hua Y, Keep RF, Hoff JT, Xi G. Intracerebral hemorrhage: Effects of aging on brain edema and neurological deficits. Stroke. 2004;35:2571–2575 [PubMed: 15472083]
31. Khandelwal S, van Rooijen N, Saxena RK. Reduced expression of cd47 during murine red blood cell (rbc) senescence and its role in rbc clearance from the circulation. Transfusion. 2007;47:1725–1732 [PubMed: 17725740]
32. von Bernhardi R, Tichauer JE, Eugenin J. Aging-dependent changes of microglial cells and their relevance for neurodegenerative disorders. J Neurochem. 2010;112:1099–1114 [PubMed: 20002526]
33. Lan X, Han X, Li Q, Li Q, Gao Y, Cheng T, et al. Pinocembrin protects hemorrhagic brain primarily by inhibiting toll-like receptor 4 and reducing m1 phenotype microglia. Brain Behav Immun. 2017;61:326–339 [PubMed: 28007523]
34. Zhou H, Zhang H, Yan Z, Xu R. Transplantation of human amniotic mesenchymal stem cells promotes neurological recovery in an intracerebral hemorrhage rat model. Biochem Biophys Res Commun. 2016;475:202–208 [PubMed: 27188654]
35. Ke K, Rui Y, Li L, Zheng H, Xu W, Tan X, et al. Upregulation of ehd2 after intracerebral hemorrhage in adult rats. J Mol Neurosci. 2014;54:171–180 [PubMed: 24664435]
36. Chistiakov DA, Killingsworth MC, Myasoedova VA, Orekhov AN, Bobryshev YV. Cd68/macrosialin: Not just a histochemical marker. Lab Invest. 2017;97:4–13

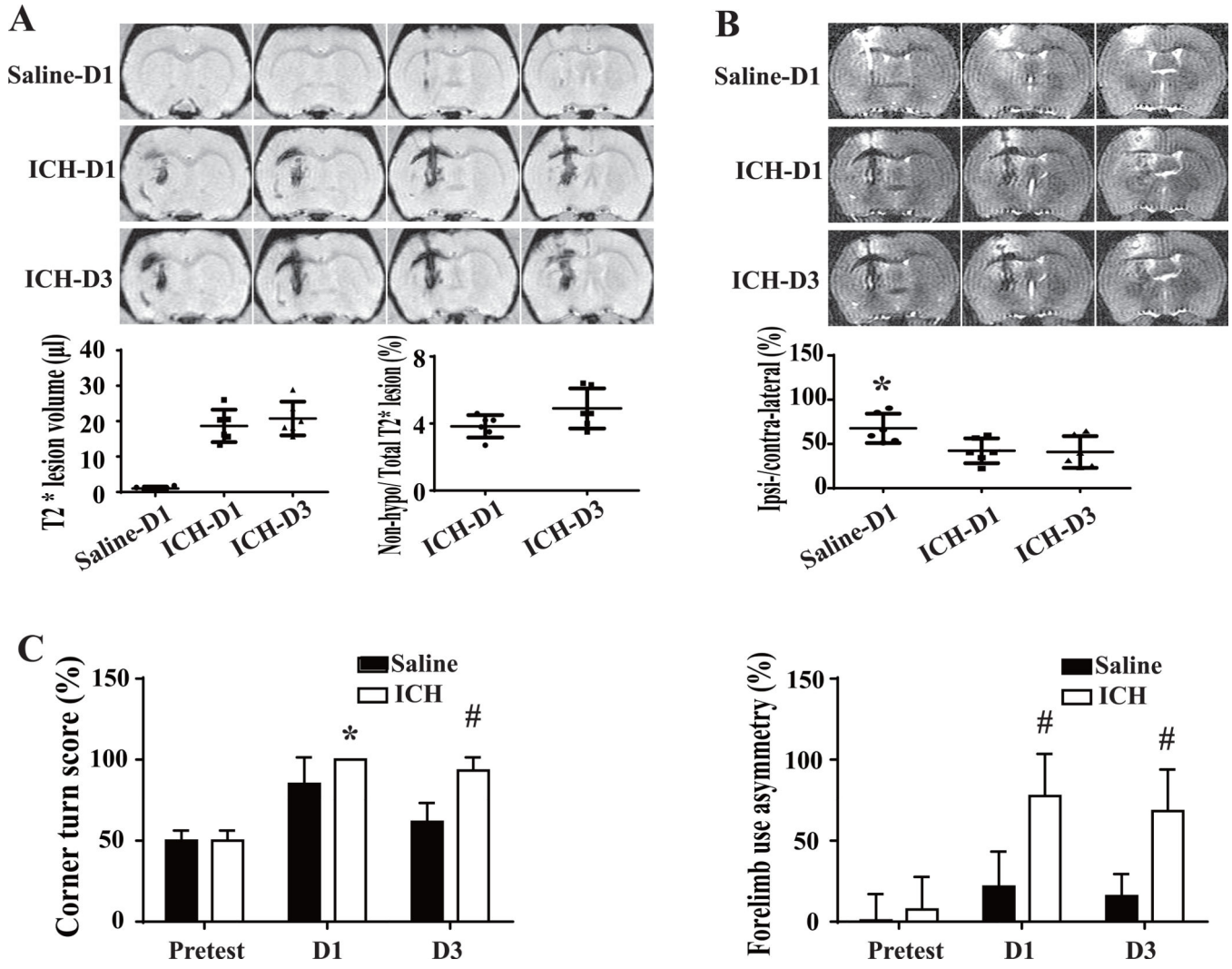

Figure 1.

The characteristics of ICH modeled by intracaudate injection of 50μl blood in aged rats. (A) Representative T2*-weighted MRI showing the hematoma volume and early hemolysis at day 1 and day 3 after ICH. Hemolysis is indicated by the non-hypointense area at the center of the hematoma. A saline-injected control is shown for comparison. (B) Brain swelling was evaluated by measuring ventricular compression on T2-weighted imaging. Ipsi/Contra = ipsilateral/contralateral ventricular volume. (C) Corner turn and forelimb use asymmetry were tested before and after ICH or saline injection. Values are means±SD; n=6 in each group, * P< 0.05 vs. other groups by one-way ANOVA; *P<0.05 and # P< 0.01 vs. saline group by two-way ANOVA.

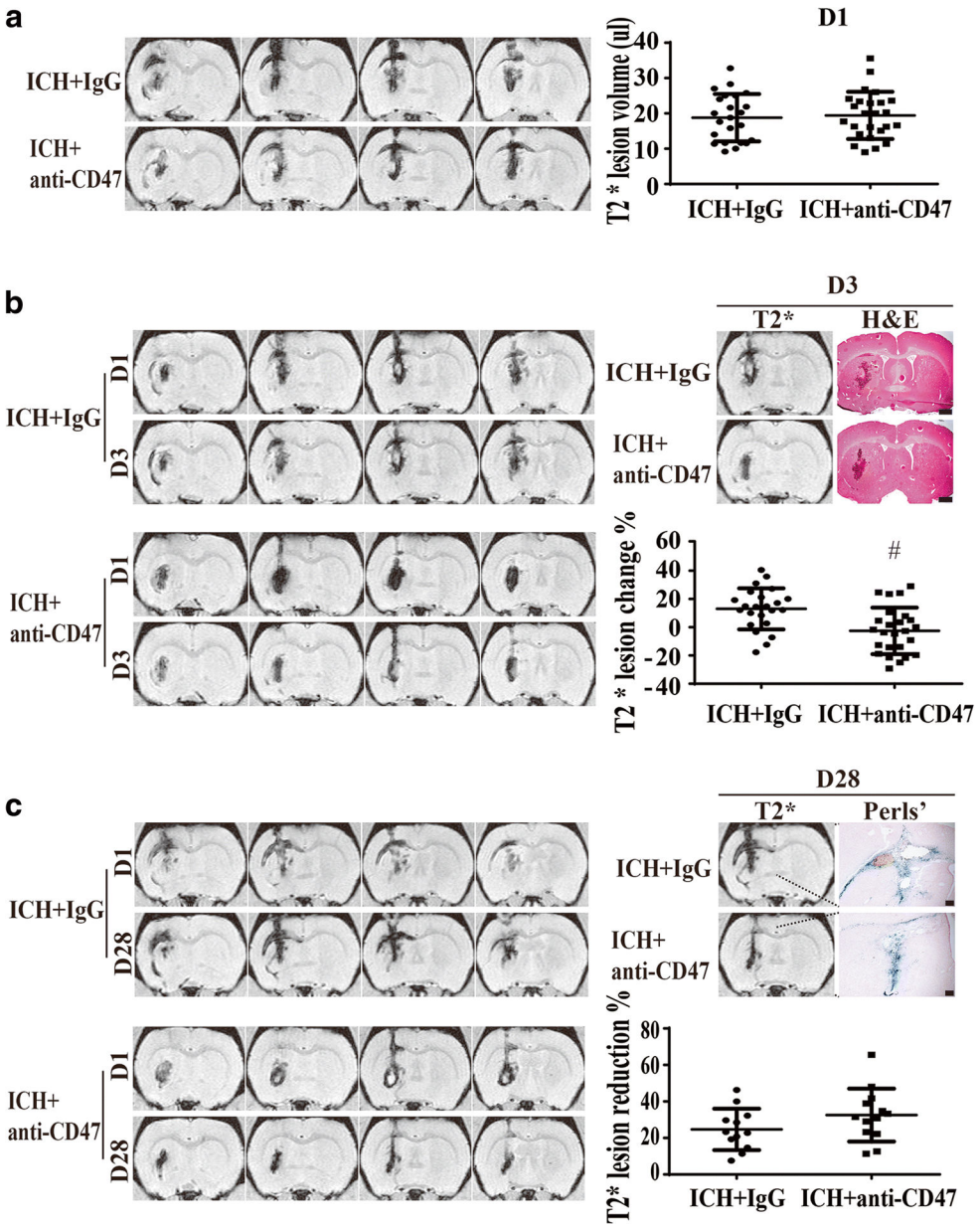

Figure 2.

Effect of CD47 blocking antibody on hematoma resolution as assessed by T2* MRI. (A) Examples of T2* MRIs at day 1 after injection of blood with anti-CD47 antibody or IgG controls. T2* lesion volumes (hematoma volumes) were calculated for the two groups. Values are mean ±SD, anti-CD47 antibody (n=25) or IgG (n=23). There was no significant difference in hematoma volume at day 1. (B) Representative examples of T2* MRIs at day 3 and a comparison between T2* lesions and H&E stain showing the T2* lesion corresponded to the hematoma at day 3. The change in T2* lesion volume (day 3 – day 1) was calculated and normalized by dividing by the day 1 volume. Values are mean±SD, scale bar= 1mm; # P< 0.01 vs. IgG group by unpaired t test; n=23 in IgG group, n=25 in anti-CD47 antibody group. (C) Representative examples of T2* MRIs at day 28 and a comparison between T2*

lesions and Perls' staining showing T2* lesion corresponded to the area of iron deposition at day 28. The change in T2* lesion volume (day 28 – day 1) was calculated and normalized by dividing by the day 1 volume. Values are mean ±SD, scale bar= 200μm; n=12 in IgG group, n=13 in anti-CD47 antibody group.

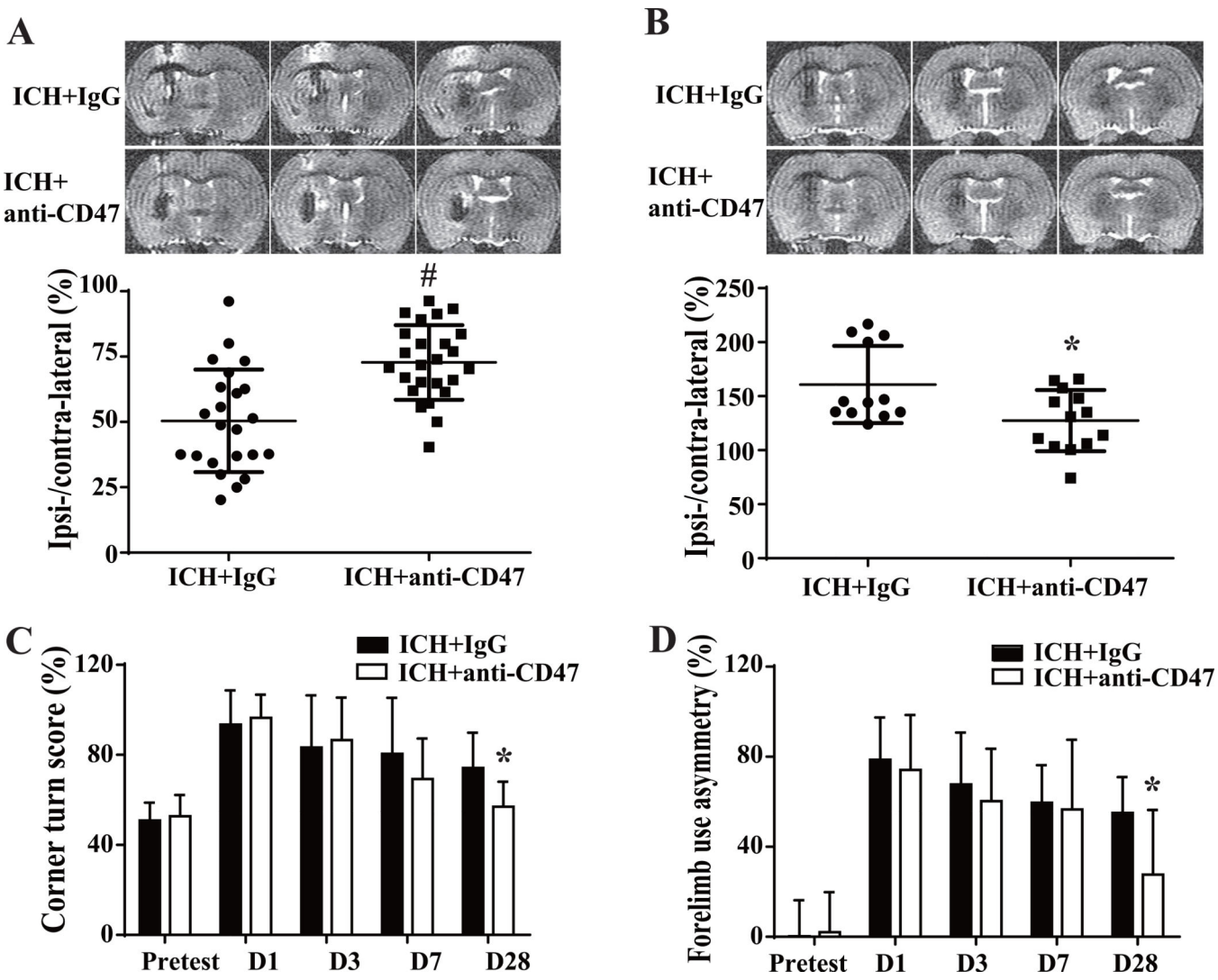

Figure 3.

Brain swelling and atrophy, neurological deficits assessment at different time points after ICH in IgG and anti-CD47 treated rats. (A) Ipsilateral ventricular compression was measured on T2 MRIs (representative images shown) to assess brain swelling at day 3 after ICH. Ipsilateral ventricular volume was expressed as a % of contralateral ventricular volume, n=23 in IgG group, n=25 in anti-CD47 antibody group. (B) Ipsilateral ventricular dilation at day 28 was measured on T2 MRIs (representative images shown) to assess brain atrophy. Ipsilateral ventricular volume was expressed as a % of contralateral ventricular volume, n=12 in IgG group and n=13 in anti-CD47 antibody group. For (A) and (B) values are means±SD; * P< 0.05, # P< 0.01 vs. IgG group by unpaired t test. (C) Corner turn and (D) forelimb use asymmetry evaluation before and after blood+IgG or blood+anti-CD47 antibody injection, n=23 in IgG group, n=25 in anti-CD47 antibody group at pretest, days 1 and 3; n=12 in IgG group, n=13 in anti-CD47 antibody group at days 7 and 28. Values are means±SD; * P< 0.05 vs. IgG group by two-way ANOVA.

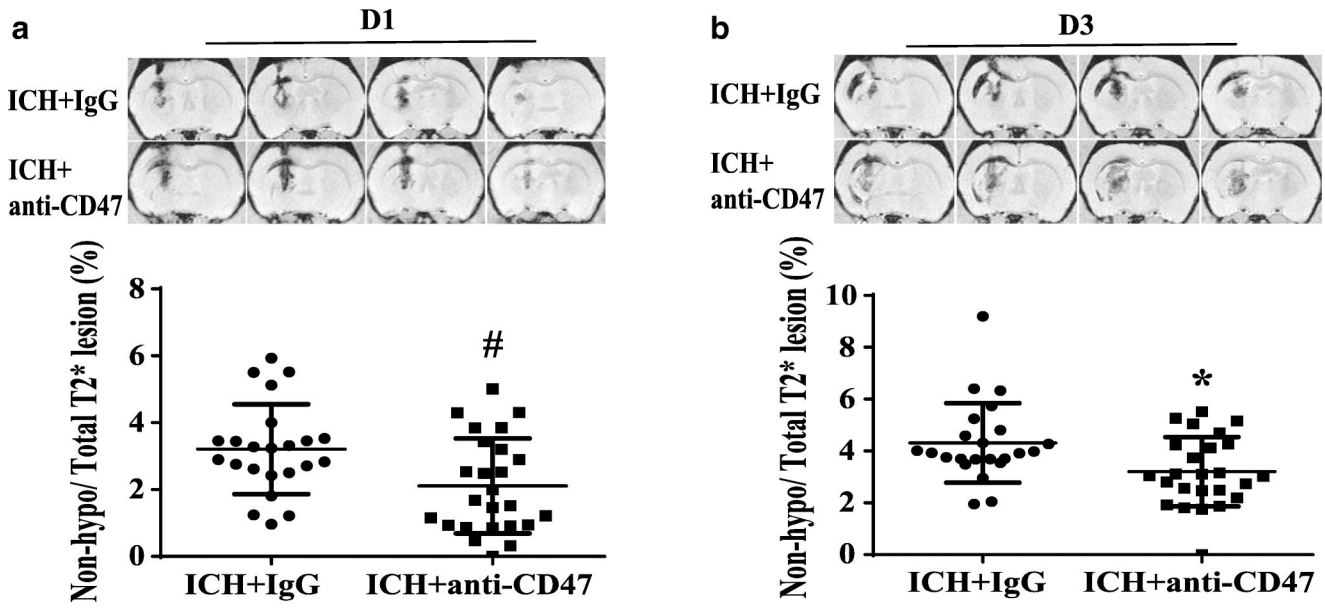

Figure 4.

Representative hemolysis in hematoma center as hyper- or iso-intense on T2* imaging at day 1 (A) and day 3 (B). Values are means ± SD; n=23 in IgG group, n=25 in anti-CD47 antibody group; * P< 0.05, # P< 0.01 vs. IgG group by unpaired t test.

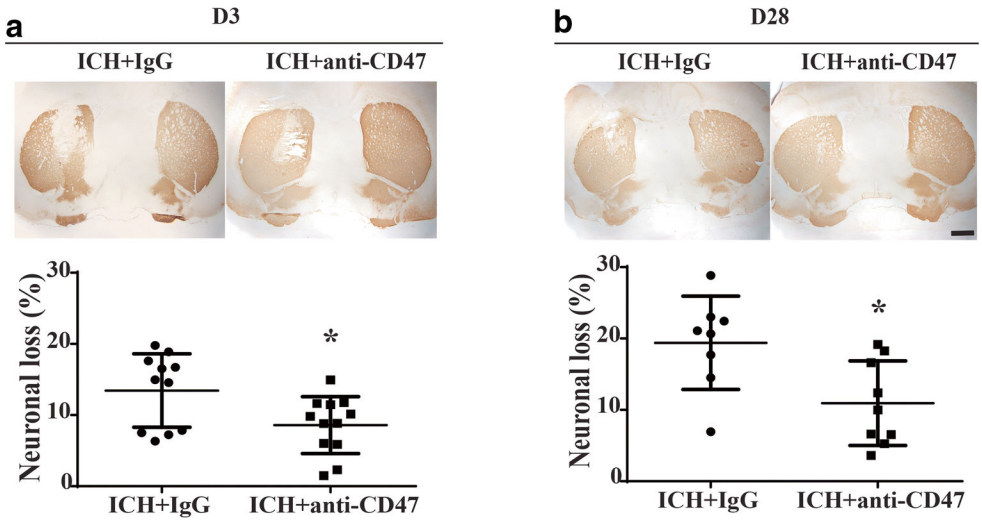

Figure 5.

Neuronal loss after ICH with and without CD47 blocking antibody treatment. (A) and (B) Examples of DARPP-32 staining in aged rats treated with IgG or anti-CD47 blocking antibody at day 3 and 28 after ICH, scale bars=1mm. Loss of DARPP-32 staining was quantified as (contralateral − ipsilateral) / contralateral DARPP-32-positive area. Values are means ± SD; n=11 in IgG group, n=12 in anti-CD47 antibody group at day 3; n=8 in IgG group, n=9 in anti-CD47 antibody group at day 28, * P< 0.05 vs. IgG group by unpaired t test.

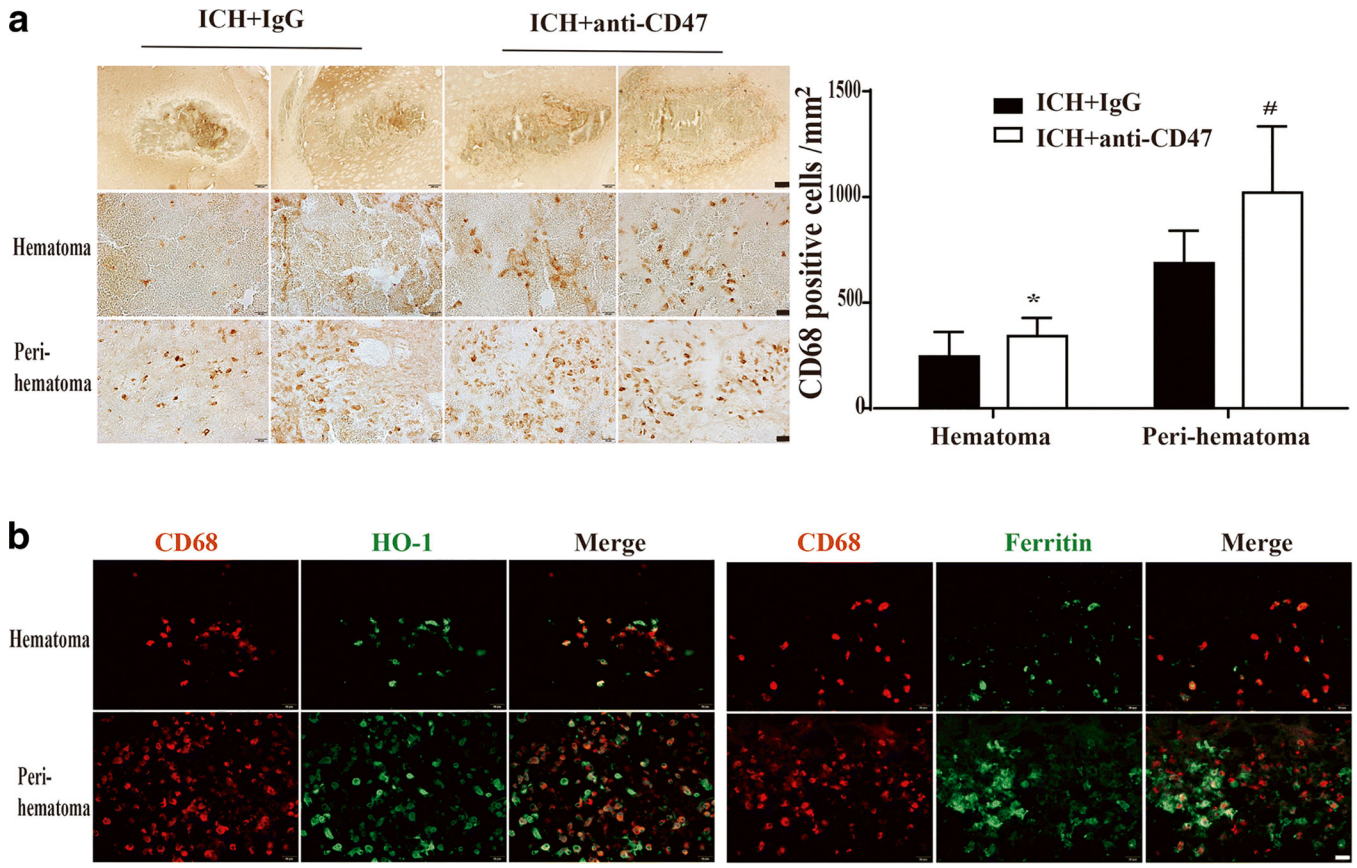

Figure 6.

Effect of CD47 blocking antibody on CD68 expression in microglia/macrophages at day 3 after ICH and co-localization of CD68 with HO-1 and ferritin. (A) Examples of CD68 immunohistochemistry from animals treated with IgG or anti-CD47 antibody; upper scale bar=200 μm and lower scale bar=20 μm. Quantification of CD68 positive cells in and around hematoma. Values are means ± SD; n=11 in IgG group, n=12 in anti-CD47 antibody group; * $P< 0.05$, # $P< 0.01$ vs. IgG group by unpaired t test. (B) Immunofluorescent double labeling of CD68 positive cells with HO-1 and ferritin positive cells in an anti-CD47 treated animal, scale bar=20 μm.